153. Protein-Loop Mimetics: A Diketopiperazine-Based Template to Stabilize Loop Conformations in Cyclic Peptides Containing the NPNA and RGD Motifs

by **Christian Bisang, Christoph Weber**[1]), and **John A. Robinson***

Institute of Organic Chemistry, University of Zürich, Winterthurerstrasse 190, CH-8057 Zürich

(3.VI.96)

We explore here an approach to mimic the structures and biological functions of protein loops in small synthetic molecules, by grafting the loop of interest onto an organic template comprising a bicyclic diketopiperazine, prepared by the formal coupling of (2*S*,4*S*)-4-aminoproline (Pro(NH_2)) and aspartic acid (Asp). The Fmoc-protected template **4** is used to prepare cyclo(-Ala[1]-Asn[2]-Pro[3]-Asn[4]-Ala[5]-Ala[6]-Temp-) (**5**) and cyclo(-Ala[1]-Arg[2]-Gly[3]-Asp[4]-Temp-) (**6**) (where Temp = template derived from **4**), containing the Asn-Pro-Asn-Ala (NPNA) and Arg-Gly-Asp (RGD) motifs. The conformational properties of these molecules are studied in aqueous solution by NMR and simulated-annealing methods. The NPNA motif, an immunodominant epitope on the circumsporozoite surface protein of the malaria parasite *Plasmodium falciparum*, is shown to adopt a stable type-I β-turn in **5**. The template in **5** adopts a preferred conformation with Pro(NH_2) $\chi_1 \approx -35°$ and the Asp moiety $\chi_1 \approx 70°$. A different template conformation is inferred for **6**, with Pro(NH_2) $\chi_1 \approx 0°$, but the ARGD loop appears by NMR to undergo rapid conformational averaging. Solid-phase binding assays reveal that **6** displays modest antagonist activity towards both the integrin $\alpha_{IIb}\beta_3$ and $\alpha_v\beta_3$ receptors.

1. Introduction. – Macromolecular recognition in nature is often mediated through functional groups displayed in loops on the surface of folded proteins. The study of loop mimetics may therefore provide access to new classes of biologically active molecules. Linear peptides are often unsuitable as mimetics of the stable secondary structures found in proteins, because of their inherent conformational flexibility. An important goal of mimetic design is to develop methods of rigidifying peptides so that the important functional groups are properly oriented for interaction with a receptor. In the case of protein loops, one approach is to graft the sequence of interest onto a relatively rigid, organic template, so generating a cyclic molecule with the desired conformational properties. This method has been used recently, *e.g.*, in the design of ligands for the integrin superfamily of cell adhesion receptors, which recognize protein ligands, such as fibrinogen, containing the amino-acid sequence Arg-Gly-Asp (RGD). Small template-bound RGD-based cyclic peptides have been discovered which act as antithrombotic antagonists of integrin receptors [1–6].

Another area where small molecule protein mimetics may be valuable is in the design of synthetic peptide vaccines [7]. Here the structural rigidity of a peptide should be optimized to mimic the conformation of protein epitopes that are important for protective antibody production. For example, linear and cyclic peptides are currently under

[1]) Present address: Department of Molecular Biology MB2, The Scripps Research Institute, 10666 North Torrey Pines Rd., La Jolla, CA 92037, USA.

investigation as potential vaccines against the malaria parasite *Plasmodium falciparum* [8] [9], HIV-1 and HTLV-1 retroviral infections [10], schistosomiasis [11] and foot-and-mouth disease virus [12], amongst others, as well as for use as contraceptive vaccines [13].

Common strategies for rigidifying peptides by cyclization include Cys-Cys disulfide bond formation (see **1**), or cyclization through the peptide backbone (**2**). However, the disulfide link in **1** introduces seven rotatable covalent bonds[2]), and the dipeptide link in **2** introduces four rotatable bonds [5]. On the other hand, relatively rigid templates with an appropriate geometry may more effectively stabilize conformations populated in the protein of interest. Of course, the template itself, as well as the amino-acid sequence, may have a significant influence on the preferred backbone conformation of the peptide loop.

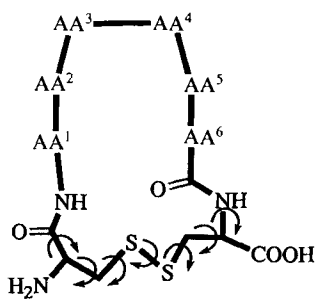

1

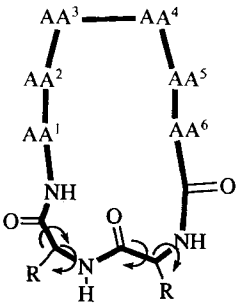

2

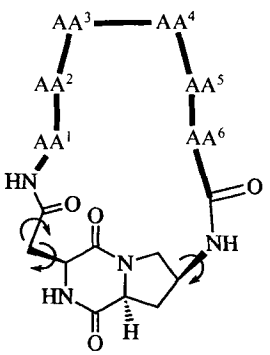

3_6

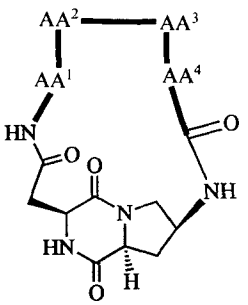

3_4

We describe below the synthesis of a new bicyclic diketopiperazine-based template and explore its use in the production of conformationally defined molecules of type $\mathbf{3}_4$ and $\mathbf{3}_6$. The Fmoc-protected template **4** has been synthesized starting from (2*S*,4*R*)-4-hydroxyproline and used to prepare the cyclic peptides **5** and **6** by a combination of solid- and solution-phase peptide synthesis (Fmoc = (9*H*-fluoren-9-yl)methoxycarbonyl). The conformational behaviour of **5** and **6** was investigated in aqueous solution by ^{1}H-NMR spectroscopy and restrained simulated annealing.

---

[2]) As pointed out by a referee, however, the disulfide link itself exhibits a strong preference for torsion angles of ~ 90°, and so will exert an influence on preferred loop conformations.

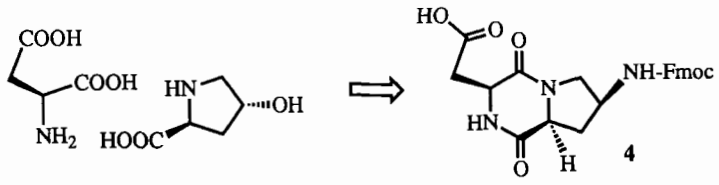

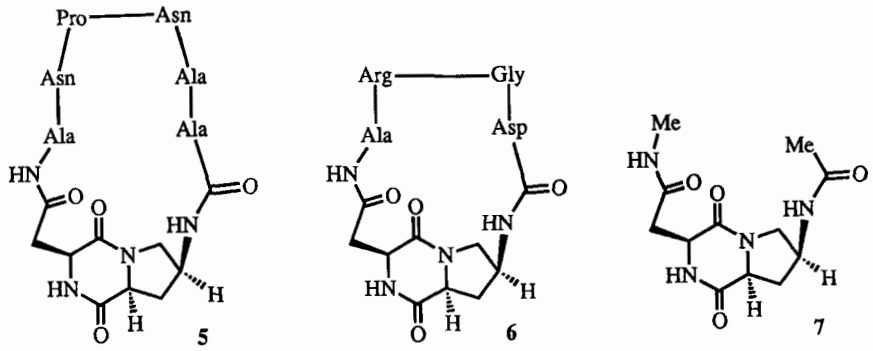

2. Results and Discussion. – 2.1. *Design.* The cyclic peptide **5** contains the Asn-Pro-Asn-Ala (NPNA) motif, which, in a tandemly repeated form, constitutes the immunodominant epitope in the circumsporozoite surface (CS) protein of the malaria parasite *Plasmodium falciparum*. Earlier studies had shown that this tetrapeptide motif has a tendency to adopt type-I β-turns in aqueous solution in linear peptides containing tandemly repeated NPNA sequences [14], and that these turns may be stabilized upon substituting proline by (*S*)-α-methylproline (P^{Me}) [15]. This secondary structure also appears to be important for immune recognition of the folded CS protein [15].

We, therefore, set out to determine whether a β-turn could be stabilized in the NPNA motif in a cyclic peptide of type $\mathbf{3}_6$. The synthesis of a six-residue loop, with two alanines flanking the NPNA motif, was undertaken to allow the NPNA motif to adopt a turn within a β-hairpin loop (see *Fig. 1*). The required geometry of the terminal peptide amide bonds can only be maintained when $4n + 2$ (n = an integer) amino-acid residues are grafted onto the template; $4n$ residues would require either both amide planes in **7** to be rotated through *ca.* 180°, which is energetically unfavourable, or a major change in loop conformation. Cyclic peptide **6**, on the other hand, contains the integrin receptor recognition sequence RGD, and was chosen as a four-residue loop mimetic since there exists, for comparison purposes, a growing body of structural and biological data on related cyclic RGD peptides [1–6].

2.2. *Synthesis.* The template **4** was prepared *via* **8**–**10** by the straightforward route shown in *Scheme 1*. The relative configuration of **4** follows from the absolute configurations of the starting materials and the inversion of configuration expected during the incorporation of the phthalimide (PhthN) moiety in a *Mitsunobu* reaction [17]. However, the configuration was confirmed upon analysis of ROESY spectra of the products **5** and **6**.

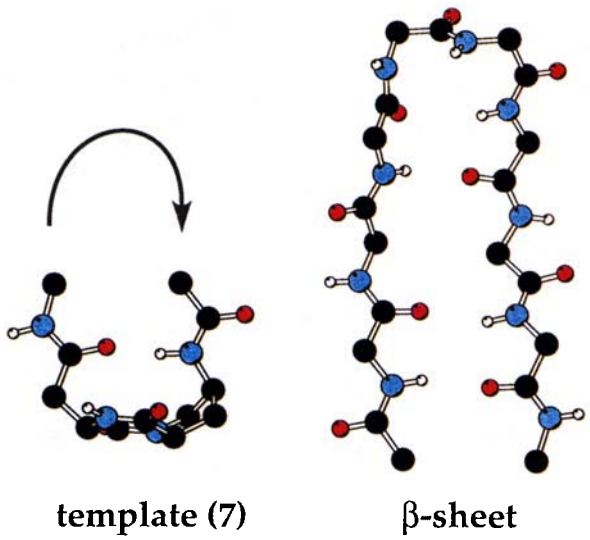

Fig. 1. *Low-energy conformation of* **7** *next to a portion of a β-hairpin loop* (residues 27–36 in the structure of toxin α from *Naja nigricollis* venom [16]). Only the backbone C(α), C'O, and NH atoms are shown; side chains and other H-atoms are omitted for clarity. C = black, N = blue, O = red.

Scheme 1

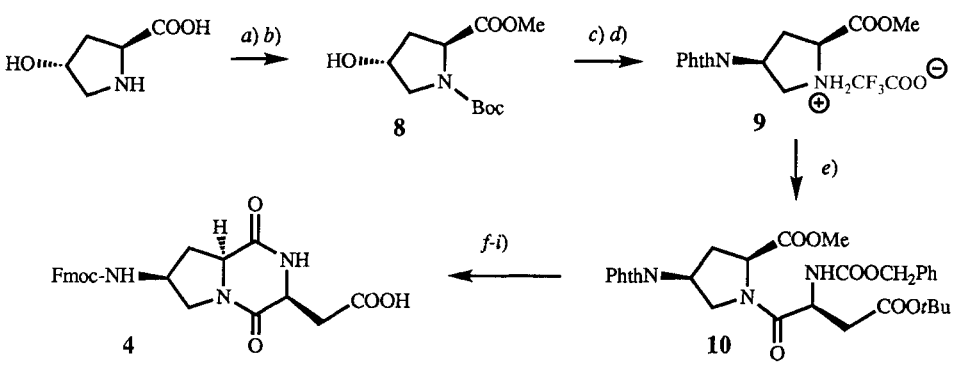

a) $SOCl_2$, MeOH; 93%. *b*) $(Boc)_2O$, Et_3N, 4-(dimethylamino)pyridine, CH_2Cl_2; 89%. *c*) PhthNH, EtOOCN=NCOOEt, PPh_3, THF. *d*) 10% CF_3COOH/CH_2Cl_2; 49%. *e*) Z-Asp (^{t}Bu)-OH, HBTU, HOBt, $^i Pr_2EtN$, DMF; 91%. *f*) H_2, Pd/C, DMF; 82%. *g*) NH_2NH_2, EtOH. *h*) Fmoc-Cl, aq. Na_2CO_3, dioxan; 94%. *i*) 5% H_2O/CF_3COOH; *ca.* 100%.

For the synthesis of **5**, *Sasrin*™ resin [18] was used, according to the route shown in *Scheme 2*. After assembly of the linear peptide **11** on the solid phase using Fmoc chemistry, the product **12** was cleaved from the resin, without removal of side-chain protecting groups. Cyclization of **12** was then performed in dilute DMF solution, with TPTU and HOBt for activation [19]. The cyclic product was obtained in 15% (unoptimized) yield. The side-chain protecting groups were then removed with CF_3COOH in the presence of scavengers, and **5** was purified by HPLC. For the synthesis of **6**, the linear peptide

H-Arg(Pmc)-Gly-Asp(ᵗBu)-Temp-Ala-O-*Sasrin* (Temp = template; Pmc = 2,2,5,7,8-pentamethylchroman-6-sulfonyl) was constructed, cleaved from the resin, cyclized and deprotected, as for **5** (see *Exper. Part*).

Scheme 2[a])

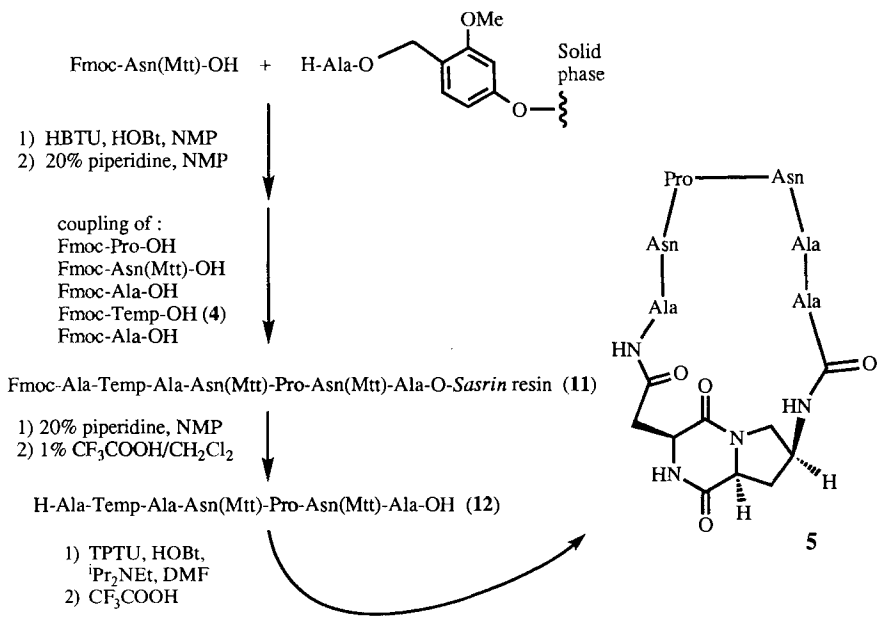

[a]) Abbreviations: Fmoc = (9*H*-fluoren-9-ylmethoxy)carbonyl, Mtt = 4-methyltrityl, HBTU = 2-(1*N*-benzotriazol-1-yl)-1,1,3,3-tetramethyluronium hexafluorophosphate, HOBt = 1-hydroxy-1*H*-benzotriazol, NMP = 1-methylpyrrolidin-2-one, TPTU = 2-(1,2-dihydro-2-oxopyridin-1-yl)-1,1,3,3-tetramethyluronium tetrafluoroborate.

2.3. *NMR Studies.* All ^{1}H-NMR spectra of **5** and **6** were recorded in aqueous solution (10% D_2O/H_2O or D_2O (99.8%)) at pH 5.0 and 300 K. The δ(H)'s and line widths were examined over the concentration range 10.0–0.1 mM. Since no significant changes were observed in these parameters, it seems likely that **5** and **6** do not aggregate under these conditions. The ^{1}H-NMR chemical-shift assignments for each peptide are given in *Tables 1* and *2*.

2.4. *Peptide* **5**. *General.* The amide region of the ^{1}H-NMR spectrum of peptide **5** revealed the presence of a minor conformer, representing *ca.* 8% of the major conformer. Chemical exchange between the major and minor forms can be seen as cross-peaks in ROESY spectra with the same positive sign as the diagonal peaks, whereas ROE cross-peaks are of negative sign. A full assignment for the minor form was not possible due to spectral overlap, and only the major form is discussed in detail below.

Stereospecific assignment of the 2 H–C(β) in the (2*S*,4*S*)-4-aminoproline (Pro(NH_2)) ring in **5** was possible on the basis of strong NOE connectivities between the *pro-S* H–C(β) and H–C(α) and H–C(γ). The two diastereotopic H–C(δ), however, could not be stereospecifically assigned. A stereospecific assignment of the 2 H–C(β) in the aspartate moiety of the template was achieved using HABAS [20].

Table 1. *^{1}H-NMR* (600 MHz) *Chemical Shifts for* **5** *at 300 K in 10% $^2H_2O/H_2O$ at pH 5.0*

Residue	Chemical shift [ppm][a])			
	NH	H–C(α)	$CH_2(\beta)$[b]) or Me(β)	Others
Ala[1]	8.33 8.07[c])	4.27	1.31	
Asn[2]	8.13 7.79[c])	4.92	2.65, 3.02	7.50 (NH, (*E*)); 7.07 (NH, (*Z*))
Pro[3]		4.43	1.95, 2.31	1.98, 2.02 $CH_2(\gamma)$); 3.76 ($CH_2(\delta)$)
Asn[4]	8.38 8.46[c])	H_2O[d])	2.73, 2.90	7.64 (NH, (*E*)); 6.98 (NH, (*Z*))
Ala[5]	7.73 8.49[c])	4.34	1.32	
Ala[6]	8.19 7.97[c])	4.27	1.33	
$Pro(NH_2)^7$[e])	8.25 7.71[c])	4.49	*1.95, 2.72*	4.61 (H–C(γ)); 3.69, 3.74 ($CH_2(\delta)$)
Asp[8]	8.34 n.d.[c])	4.44	*2.79, 3.22*	

[a]) Chemical shifts are measured relative to internal TSP (sodium 3-(trimethylsilyl)(D_4)propanoate). $Pro(NH_2)^7$ and Asp[8] are the aminoproline and aspartate moieties of the template. [b]) Stereospecific assignments are in *italics*, in the order *pro-R, pro-S*. [c]) Peptide NH assignment for the minor conformer. [d]) Resonance lies under the signal of H_2O. [e]) The $Pro(NH_2)^7$ NH refers to NH–C(γ).

Table 2. *^{1}H-NMR* (600 MHz) *Chemical Shifts for* **6** *at 300 K in 10% $^2H_2O/H_2O$ at pH 5.0*

Residue	Chemical shift [ppm][a])			
	NH	H–C(α) or $CH_2(\alpha)$	$CH_2(\beta)$[b]) or Me(β)	Others
Ala[1]	8.31	4.14	1.40	
Arg[2]	8.28	4.28	1.78, 1.93	1.60, 1.63 ($CH_2(\gamma)$); 3.22 ($CH_2(\delta)$); NH 7.26; NH_2 6.66
Gly[3]	8.01	3.76, 4.10		
Asp[4]	8.23	4.55	2.64, 2.82	
$Pro(NH_2)^5$[c])	7.66	4.47	*2.38, 2.61*	4.44 (H–C(γ)); 3.56 (H–C(δ_3)); 3.90 (H–C(δ_2))
Asp[6]	8.29	4.47	*2.86, 3.21*	

[a]) Chemical shifts are measured relative to internal TSP. $Pro(NH_2)^7$ and Asp[6] are the aminoproline and aspartate moieties of the template. [b]) Stereospecific assignments are in *italics*, in the order *pro-R, pro-S*. [c]) The $Pro(NH_2)^5$ NH refers to NH–C(γ).

Chemical Shifts of **5**. A consistent trend observed in H–C(α) and NH chemical shifts in regular secondary structure in proteins is an upfield shift on helix formation and a downfield shift on β-sheet formation [21–23]. While the origins of these effects are still a matter of debate, one of the principal determinants of the amide NH chemical shift appears to be the H-bond [22]. In **5**, all peptide NH protons are shifted upfield from the random coil values (taken from the values of *Merutka et al.* [24], at pH 5, corrected to 300 K), but the shift is most striking for Ala[5] NH (+0.75 ppm). Our structure calculations (*vide infra*) place this NH in a likely H-bonding position with the Asn[2] peptide CO group, across a β-turn. It is interesting to note that a shift of similar magnitude was observed for the Ala

NH in linear peptides containing tandemly repeated NP^{Me}NA motifs [15], which adopt highly populated β-turn conformations in aqueous solution. In this β-turn motif, the NH of Ala (i+3) is H-bonded to the Asn (i) peptide CO group. In linear peptides containing the NPNA motif [14], where this β-turn is less frequently populated, the NH of Ala in the i+3 position also resonates upfield of the random-coil value to the extent of *ca.* +0.5 ppm.

The temperature coefficients of amide NH δ(H)'s are shown in *Table 3*. The value of −2.9 ppb/K for the Ala^5 NH in **5** is significantly below the random-coil value for Ala (−8.2 ppb/K) [24], consistent with partial protection of this NH from solvent, and its possible involvement in an intramolecular H-bond (*vide infra*). Low temperature coefficients (in the range −1.5 to −2.6 ppb/K) were also seen for Ala at the i+3 position in the NP^{Me}NA motif [15]. The temperature coefficient for Asn^4 NH in **5** is also slightly lowered from the random-coil value (*ca.* −7.0 ppb/K).

Table 3. *Temperature Coefficients for* **5** *and* **6**

	Temperature coefficients[a]) for **5**										
Residue	Ala^1	Asn^2	NH(E)	NH(Z)	Asn^4	NH(E)	NH(Z)	Ala^5	Ala^6	Pro(NH$_2$)	Asp^8
$-\Delta\delta$/K [ppb/K]	7.3	6.0	3.9	5.8	5.0	6.3	5.8	2.9	5.7	6.0	7.5

	Temperature coefficients[a]) for **6**					
Residue	Ala^1	Arg^2	Gly^3	Asp^4	Pro(NH$_2$)^5	Asp^6
$-\Delta\delta$/K [ppb/K]	8.6	7.9	0.4	4.1	5.9	7.2

[a]) The coefficients for the peptide amide NH's and the side-chain NH's of Asn^2 and Asn^4 are given. Measurements were made in aqueous solution (see text) in the range 5–30°.

Amide Proton Exchange in **5**. Peptide amides involved in intramolecular H-bonding, or otherwise shielded from solvent, can be identified by their relatively slow rate of H/D exchange. It is generally accepted that intramolecular H-bonds in proteins must break before exchange with the solvent can occur [25] [26]. In this work, slowly exchanging amide NH's were detected by dissolving **5** in D_2O and monitoring signal intensities of residual amide NH resonances at pD* 3.5 and 18°. No significant changes in chemical shifts or temperature coefficients were observed as the pD* was lowered from 5 to 3.5. As shown in *Fig. 2*, the Ala^5 NH exchanges more slowly than those of Ala^1, Asn^2, and Ala^6, with Asn^4 NH showing an intermediate rate of exchange. The amide temperature coefficients (*vide supra*) and the peptide amide exchange rates thus provide complementary evidence that Ala^5 NH is involved in intramolecular H-bonding. The same parameters suggest that the Asn^4 peptide amide may also populate intramolecular H-bonds, but to a lesser extent than does Ala^5 NH.

Coupling Constants of **5**. In peptides and proteins, $^3J(\alpha,NH)$ values between 8.0 and 6.5 Hz are often considered consistent with conformational averaging [27]. $^3J(\alpha,NH)$ coupling constants for **5** measured from 1D and E.COSY spectra are shown in *Table 4*. Only the Asn^4 $^3J(\alpha,NH)$ = 8.8 Hz lies outside this middle range, and has a value typical (*ca.* 9 Hz) for residue (i+2) in type-I β-turns in proteins [28].

The combination of large and small $^3J(\alpha,\beta)$ coupling constants for Asn^2 and Asn^4 are indicative of preferred side-chain conformations. Unambiguous stereospecific assignments for these Asn H–C(β)'s could not be obtained using the program HABAS [20].

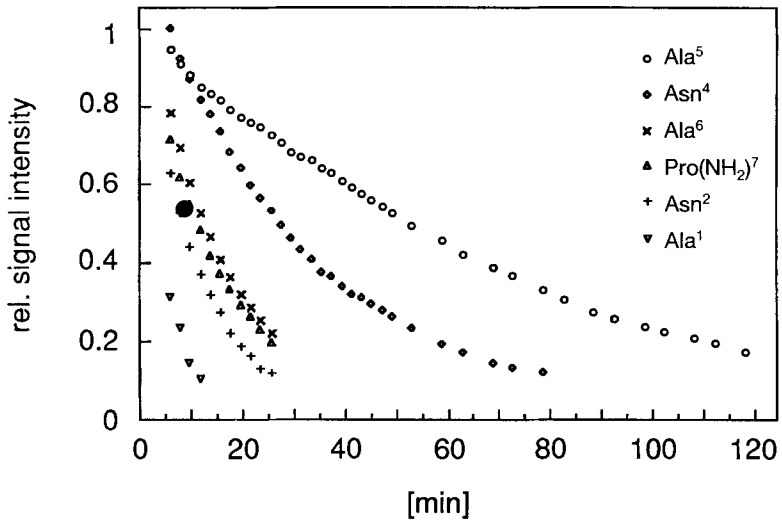

Fig. 2. *H/D Exchange of peptide amide protons in* **5** (see text). Each point represents the residual signal intensity *vs.* time.

Table 4. *^{1}H-NMR Coupling Constants*[a]) [Hz] *for* **5**

Residue	$^3J(\alpha,NH)$	$^3J(\alpha,\beta)$	Others
Ala[1]	6.0	7.4	
Asn[2]	7.3	4.3, 9.6[b])	$J(\beta,\beta')$ = 15.0
Pro[3]	–	5.3, 9.1[b])	n.d.
Asn[4]	8.8	9.7, 5.3[b])	$J(\beta,\beta')$ = 15.2
Ala[5]	6.7	6.7	
Ala[6]	6.3	6.8	
Pro(NH$_2$)[7]	8.2[c])	10.7, 7.1[d])	$J(\beta_2,\gamma)$ = 8.1, $J(\beta_3,\gamma)$ = 7.3, $J(\beta,\beta')$ = 12.3, $J(\gamma,\delta)$ = 5,9[b]), $J(\gamma,\delta')$ = 8.6[b]), $J(\delta,\delta')$ = 12.7, $J(\alpha,\alpha')$ = 2.5[e])
Asp[8]	< 3.0	5.0, 2.7[d])	$J(\beta,\beta')$ = 16.8

[a]) Measured from 1D and/or E.COSY spectra.
[b]) Stereospecific assignments not available.
[c]) Refers to the ^3J(NH–C(γ), H–C(γ)) coupling.
[d]) Given in the order *pro-R*, *pro-S*.
[e]) $J(\alpha,\alpha')$ = ^5J(H,H) of Pro(NH$_2$)[7] H–C(α) to Asp[8] H–C(α) (see text).

However, these $^3J(\alpha,\beta)$ values are very similar to those observed earlier for Asn residues at equivalent positions in linear peptides containing tandemly repeated NP^{Me}NA motifs [15], indicating a similar side-chain conformational bias in **5**.

The pyrrolidine ring of Pro(NH$_2$) in the template is likely to prefer a folded (envelope or twist) conformation [29–31]. Three models representing energy-minimized Pro(NH$_2$) ring puckers are shown in *Fig. 3*, along with ranges of predicted ^3J(H,H) coupling constants for each conformer. The latter were obtained using the dihedrals shown and coefficients for the *Karplus* curve derived for χ angles in amino-acid side chains [32]. However, the ^3J(H,H) coupling constants will deviate from these ranges if twist forms are

populated or flattening of the ring pucker occurs. Nevertheless, the occurrence of these ring puckers (or close relatives) should be straightforward to identify, based on the appearance of small (< 4 Hz) or large (> 9 Hz) ^3J values, whereas rapid ring flipping should give rise to averaged coupling constants in the range *ca.* 5–8 Hz. Recent NMR studies of proline-ring conformations in a cyclic peptide [33] and in proteins [34] have shown that both $^3J(\alpha,\beta)$ coupling constants in the range 5–8 Hz are characteristic of proline-ring flips. The $^3J(\alpha,\beta)$ values observed for the *cis*-4-aminoproline moiety in **5** (*Table 4*) indicate a preferred ring pucker similar to conformer **I** in *Fig. 3* ($\chi_1 \approx -35°$) [31], which places the 4-amido substituent in an equatorial position. However, the $^3J(\beta,\gamma)$ and $^3J(\gamma,\delta)$ values deviate from those expected for conformer **I**, perhaps for the reasons mentioned above. For the aspartate moiety of the template, two small $^3J(\alpha,\beta)$ coupling constants are observed, clearly indicating a preferred χ_1 torsion angle of *ca.* +70°, similar to that shown in **7** (*Fig. 1*). Finally, the observed $^5J(\alpha,\alpha')$ homoallylic coupling (*Table 4*) is well precedented and indicates a significant folding of the diketopiperazine ring [35] [36].

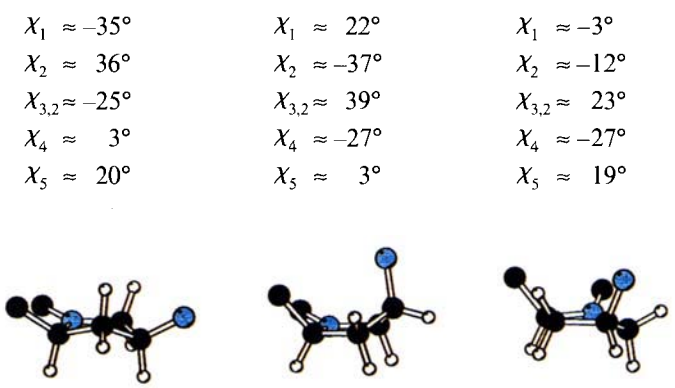

	I	II	III
$^3J(\alpha,\beta_2)$, $^3J(\alpha,\beta_3)$	11–13, 5–7	2–3, 7–9	5.2–6.5, 8.5–10.5
$^3J(\beta_2,\gamma)$, $^3J(\beta_3,\gamma)$	11–13, 5–7	1.5–2.5, 5–7	3–4, 8.2–10.2
$^3J(\gamma,\delta_2)$, $^3J(\gamma,\delta_3)$	9.7–11, 6.5–8.5	1.5–2.5, 5–7	1.5–3, 7–9

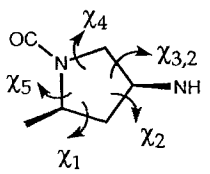

Fig. 3. *Three low-energy ring puckers for a (2S,4S)-4-aminoproline moiety, with the $^3J(H,H)$ coupling constants expected for each* (see text). Pucker **I**, C(β) up (*i.e.*, above the plane defined by the other four ring atoms); pucker **II**, C(γ) up; pucker **III**, C(δ) down. C = black, N = blue. The low energy conformations were found in a conformational search performed on **7**.

NOE's of **5**. For the analysis of NOE connectivities, a series of ROESY spectra were recorded with mixing times (spin lock periods) of 75, 150, 225, 300 and 375 ms. A summary of observed NOE's is shown in *Fig. 4*. Noteworthy, are the medium range (i, $i+2$) and (i, $i+3$) NOE connectivities within the four residues of the NPNA motif, as well as a strong Asn^4-Ala^5 $d(NH^i,NH^{i+1})$ NOE, which are characteristic of a highly populated β-turn conformation with proline at the ($i+1$) position. The NOE data, therefore, complement the amide NH temperature coefficients, the H/D exchange data and the pattern of ^3J coupling constants, described above, in pointing to highly populated β-turn conformations within the NPNA unit in **5**, most likely similar to β-turns found in linear peptides containing tandemly repeated NP^{Me}NA motifs [15].

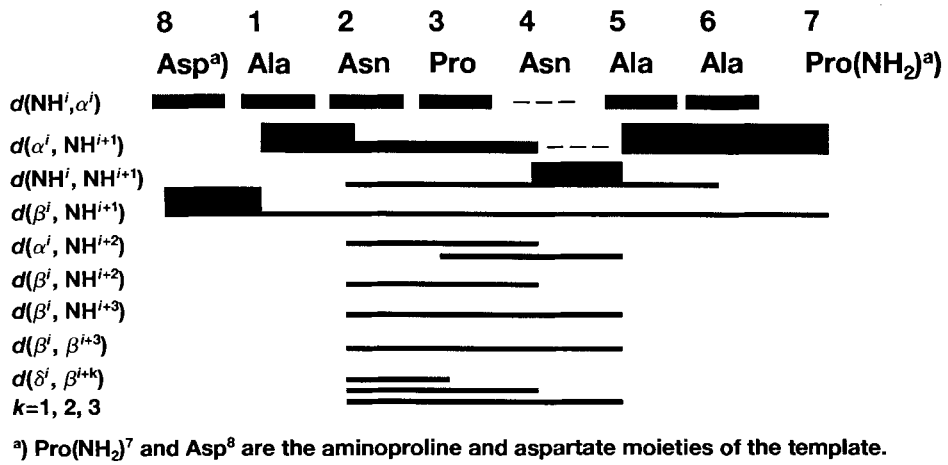

[a]) **Pro(NH$_2$)^7 and Asp^8 are the aminoproline and aspartate moieties of the template.**

Fig. 4. *Summary of NOE connectivities found for* **5** *at 300 K.* Data are from ROESY spectra with a spin-lock period of 300 ms. NOE Connectivities with Pro^3 are to the H–C(δ)'s in place of NH. Pro(NH$_2$)^7 NH refers to the NH–C(γ).

Structure Calculations for **5**. Since the NMR data point to a preferred conformation for **5**, attempts were made to deduce average solution conformations, using distance restraints derived from NOE connectivities in structure calculations with the simulated annealing (SA) method [37] (see *Exper. Part*). Using 58 upper-distance and two dihedral-angle restraints, the calculations yielded 25 out of 50 SA structures that have no NOE violations > 0.1 Å, and all of which lie within 3 kcal/mol of the lowest-energy conformer (see *Table 5*). The two dihedral-angle restraints used restrict Asp^8 χ_1 to the range 30 to 90°, and Pro(NH$_2$)^7 χ_1 to between -50 and -10°, as implied by the observed $^3J(\alpha,\beta)$ coupling constants (*vide supra*).

The calculated structures seem to fall into two tightly clustered groups, which are themselves closely related (*Fig. 5*). Within the limited accuracy of the NMR-derived structural constraints, all calculated structures fulfill the input restraints equally well, and this apparent clustering may, therefore, be purely artefactual. In fact, other NMR parameters indicate significant residual flexibility in **5** (*vide infra*). A superimposition of these 25 SA structures reveals good convergence at a pairwise r.m.s. deviation for the

backbone N, C(α), and C′ atoms in all residues (including template) of 0.12 ± 0.22 Å. Superimposition of the N, C(α), and C′ backbone atoms of the NPNA motif yields an r.m.s. deviation of only 0.10 ± 0.14 Å (see *Fig. 5*). The lowest-energy structure is depicted in *Fig. 6*.

Table 5. *Summary of Input Restraints for the Structure Calculations and the Violations, r.m.s. Deviations, and Energies of the Final 25 Structures*

Input to structure calculations		*Results of structure calculations*[a])		
^{1}H,^{1}H-distance restraints		Energy [kcal/mol]		
total	58	total	86.12 ± 0.61	85.74..88.05
intra-residue	28	nonbond	37.39 ± 1.27	36.06..41.18
sequential	21	restraint	0.51 ± 0.04	0.39.. 0.62
medium-range	9	NOE violations		
dihedral-angle restraints	2	number > 0.1 [Å]	0	
total restraints/residue	7.5	maximum [Å]	0.076 ± 0.011	0.043..0.095
		sum [Å]	0.193 ± 0.045	0.046..0.232
		Pairwise r.m.s.deviation	0.115 ± 0.217	0.000..0.635

[a]) Results are listed as average ± standard deviation and range of observed values (low..high).

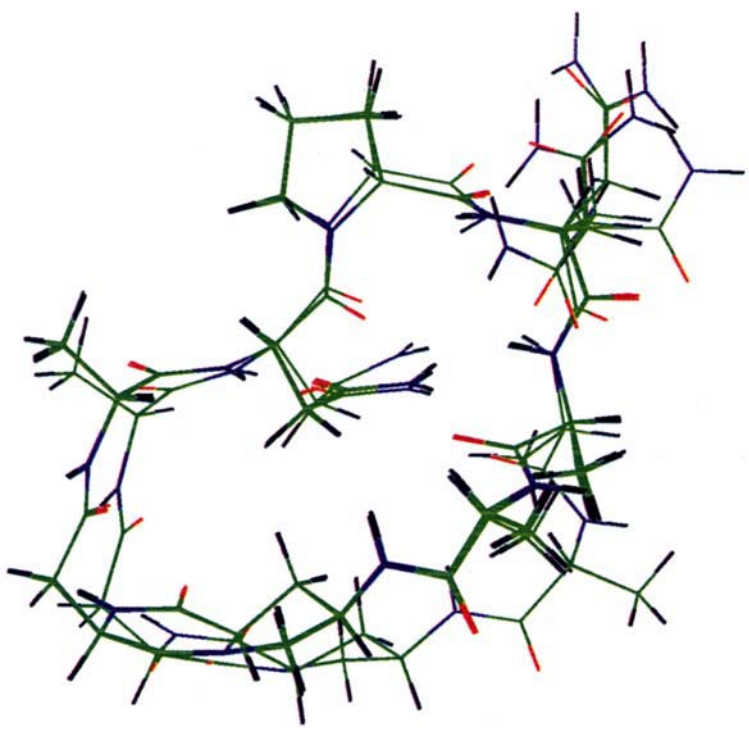

Fig. 5. *Superimposition of the final 25 SA structures of* **5**. The backbone N, C(α), and C′ atoms in the NPNA motif are superimposed (see text).

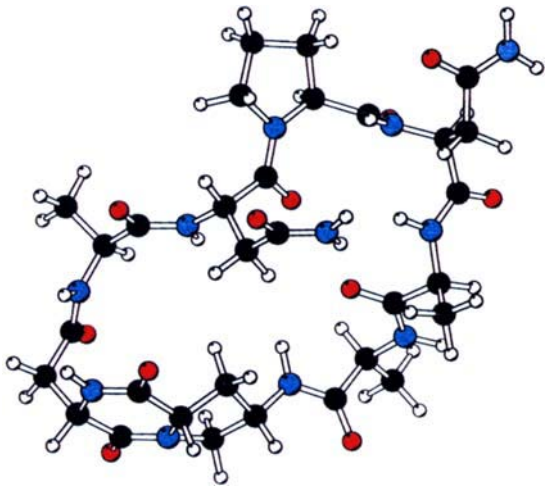

Fig. 6. *The lowest-energy SA structure derived for* **5**. C = black, N = blue, O = red.

The observed ϕ and ψ angles for Pro^3 (i+1) and Asn^4 (i+2) in the 25 SA structures approximate frequently the dihedral angles for an ideal type-I β-turn [38]. The predominance of a type-I β-turn is supported by the strong Asn^4-Ala^5 d(NH^i,NH^{i+1}) NOE (*Fig. 4*). However, flipping of the Pro^3-Asn^4 peptide bond towards a type-II β-turn could be possible since a weaker Pro^3-Asn^4 d(α^i,NH^{i+1}) NOE connectivity is also observed. Thus, the molecule may retain a significant degree of flexibility, which includes flipping of amide planes. A H-bond between the Asn^2 side-chain amide NH(E) and the Ala^5 CO was found frequently (using InsightII, *Biosym Inc.*) in the SA structures, which is also consistent with the low temperature coefficient found for this amide proton (*Table 3*). Indeed, H-bonding involving the Asn^2 side chain appears to contribute significantly to β-turn stability in this NPNA motif, as noted in earlier studies [15]. The amide temperature coefficients, relative H/D amide exchange rates, and NOE connectivities thus provide complementary and mutually supportive data suggesting that the SA structures shown in *Figs. 5* and *6* represent likely conformations for **5** in aqueous solution.

An accurate estimate of the frequency of turn population in the NPNA motif in **5** is difficult to derive. However, the magnitude of the amide-proton temperature coefficient of the (i+3) residue in the turn can be used to give an estimate of the population of intramolecular H-bonded conformers. If it is assumed that the highest attainable temperature coefficient for the Ala amide proton is close to the random coil value of −8.2 ppb/K [24] and the lowest value, corresponding to complete intramolecular H-bond and, hence, turn formation, is close to 0 ppb/K, a linear correlation between the population of the β-turn and the temperature coefficient leads to an estimate of *ca.* 65% β-turn formation in **5**. This assumes, of course, that a direct correlation exists between such H-bond formation and turn population, which may not be the case. Similar arguments applied to linear peptides with repeating NPNA or NP^{Me}NA motifs, however, suggest fractional turn populations of *ca.* 25 and 80%, respectively [15]. On this basis, the β-turn is significantly stabilized in the context of cyclic peptide **5**, but less so than in linear peptides containing repeated NP^{Me}NA motifs.

2.5. *Peptide* **6**. *NMR Studies*. The ^{1}H-NMR spectrum of **6** reveals one major component (> 98%) on the NMR time scale. The amide chemical shift of Pro(NH$_2$)^5 (*i.e.*, the (2*S*,4*S*)-4-aminoproline moiety of the template) resonates notably upfield of the other peptide NH groups at pH 5 (*Table 2*). The shifts of most peptide NH resonances change significantly, however, over the pH range 3.5–5. Only the Pro(NH$_2$)^5 NH–C(γ) shows a relatively slow exchange rate in D$_2$O, which proceeds to completion over *ca.* 20 min at pD* 5 and 5°. The other NH's exchange completely within the few min necessary for sample preparation and measurement of a 1D ^{1}H-NMR spectrum in D$_2$O. The amide temperature coefficients, on the other hand, show a low value for the Gly^3 NH, and a close to random-coil value for Pro(NH$_2$)^5 NH–C(γ) at pH 5 (*Table 3*). These data, therefore, give conflicting indications of which amide protons might be involved in H-bonding – the Pro (NH$_2$)^5 NH–C(γ) has a high temperature coefficient but a relatively slow exchange rate, and *vice versa* for the Gly^3 NH.

Conflicting line-width and temperature-shift data have been observed during NMR studies of the linear peptide GRGDSP in aqueous solution [39], as well as in exchange rate and shift data with other cyclic peptides [40] and small proteins [41] [42]. *Andersen* and coworkers [40] suggested that amide temperature coefficients may reflect not only intrinsic NH protection from solvent, but also temperature-dependent changes in the populations of interconverting conformers when these display widely divergent NH shifts. However, H/D exchange rates may also be influenced by local electrostatic effects from neighbouring charged residues. The charged groups in Arg^2 and Asp^4 in **6** might promote Gly^3 NH exchange. The conflicting $\Delta\delta/T$ and H/D exchange data also raise the possibility that **6** may be equilibrating rapidly between diverse conformational states under the NMR conditions, a conclusion suggested also by the NOE data described below.

The $^3J(\alpha,\beta)$ coupling constants for the template in **6** are of interest (*Table 6*). Low $^3J(\alpha,\beta)$ values for the Asp^6 template side chain indicate a preferred conformation which is similar to that observed in the template in **5** with $\chi_1 \approx 60$–80° (*vide supra*). The observed $^3J(\alpha,\beta)$, $^3J(\beta,\gamma)$ and $^3J(\gamma,\delta)$ values for the Pro(NH$_2$)^5 pyrrolidine ring, however, suggest a preferred pucker with $\chi_1 \approx 0°$, which places the N-substituent in a pseudo-axial position, unlike that seen for **5**, but similar to that seen in conformer **III** in *Fig. 3*.

Table 6. *^{1}H-NMR Coupling Constants*[a]) [Hz] *for* **6**

Residue	$^3J(\alpha,NH)$	$^3J(\alpha,\beta)$	Others
Ala^1	3.8	7.2	
Arg^2	7.8	5.6, 9.4[b])	n.d.
Gly^3	4.1, 6.5	–	$J(\alpha,\alpha') = 17.0$
Asp^4	7.8	7.1, 5.8[b])	$J(\beta,\beta') = 16.3$
Pro(NH$_2$)^5[c])	6.4[d])	5.8, 9.5[e])	$J(\beta_2,\gamma) = 3.2$, $J(\beta_3,\gamma) = 6.4$, $J(\beta,\beta') = 14.0$, $J(\gamma,\delta_2) = 1.7$, $J(\gamma,\delta_3) = 5.6$, $J(\delta,\delta') = 12.7$, $J(\beta_2,\delta_2) = 2.2$, $J(\alpha,\alpha') = 2.3$[f])
Asp^6[c])	< 3.0	3.9, 3.5[e])	$J(\beta,\beta') = 17.3$

[a]) Measured from 1D and/or E.COSY spectra. [b]) Stereospecific assignments not available. [c]) Pro(NH$_2$)^5 and Asp^6 are the aminoproline and aspartate moieties of the template. [d]) Refers to the ^3J(NH–C(γ), H–C(γ)) coupling. [e]) Given in the order *pro-R*, *pro-S*. [f]) $J(\alpha,\alpha') = {}^5J$(H,H) of Pro(NH$_2$)^5 H–C($\alpha$) to Asp^6 H–C($\alpha$).

NOE Connectivities were determined for **6** in a series of ROESY spectra, as for **5**. However, only intra-residue and sequential NOE's were detected; NOE's between non-adjacent residues were absent. Although the NMR data are not indicative of a unique conformation for **6** in aqueous solution, the observed NOE connectivities were used to derive distance restraints for SA calculations. However, the structures generated all had significant NOE violations in the range 0.22–0.34 Å, and could not readily account for the amide temperature shift coefficients. It seems very likely that the peptide backbone of **6** is interconverting rapidly between two or more conformational states in aqueous solution, which cannot be identified in a meaningful way using this approach. More detailed studies using techniques that account for rapid averaging may help to address this point.

Biological Studies with **6**. Solid-phase binding assays for antagonist activity against immobilized platelet receptor GPIIb-IIIa ($\alpha_{IIb}\beta_3$) and the closely related vitronectin receptor ($\alpha_v\beta_3$) were performed in the laboratories of *F. Hoffmann-La Roche Ltd.*, Basel, following published procedures [43]. Peptide **6** inhibited fibrinogen binding to purified immobilized GPIIb-IIIA with an $IC_{50} \approx 250$ nM (IC_{50}(**6**)/IC_{50}(RGDS) = 0.069) and fibrinogen binding to purified and immobilized vitronectin receptor ($\alpha_v\beta_3$) with an $IC_{50} \approx 100$ nM (IC_{50}(**6**)/IC_{50}(RGDS) = 0.36), in both cases using the linear tetrapeptide RGDS as standard. Given the high conformational flexibility of **6** inferred in this work, it should be possible to develop more potent and selective integrin-receptor ligands by incorporating additional constraints into the template and/or peptide backbone.

3. Outlook. – The results described above clearly establish that the template **4** can be used to prepare cyclic protein-loop mimetics, and that in some cases the loop backbone may have a well-defined secondary structure, most likely dependent upon its length and sequence. In **5**, a highly populated type-I β-turn conformation within the NPNA motif was detected in aqueous solution. The SA structures found for **5** also show which template conformations are preferred. This information is valuable in attempts to design new loop structures with predictable conformational and biological properties. However, to further develop the usefulness of this template, work is underway to introduce additional functional groups into **4**, as handles to allow the synthesis of loop mimetics on a solid phase, and their assembly into protein-like multiple-loop arrays [44].

The authors thank the *Swiss National Science Foundation* for financial support, and Dr. *D. Obrecht*, *F. Hoffmann-La Roche Ltd.*, for arranging biological assays.

Experimental Part

General. See [45].

Methyl (2S,4R)-4-Hydroxyprolinate–Hydrochloric Acid. Thionyl chloride (45.0 g, 378 mmol) was added to a soln. of (2*S*,4*R*)-4-hydroxyproline (25.0 g, 191 mmol) in MeOH (400 ml) at 0° within 15 min and then refluxed for 4.5 h. The solvent was evaporated and the product recrystallized from Et_2O/MeOH (32.31 g, 93%). M.p. 162–164°. $[\alpha]_D^{25} = -24.3$ (*c* = 1.05, MeOH). IR (KBr): 3370*s* (br.), 3160*m*, 2950*vs* (br.), 1745*s*. ^{1}H-NMR (300 MHz, (D_6)DMSO): 9.96 (br., 2 H); 5.64 (br., 1 H); 4.45 (*dd*, *J* = 10.9, 7.4, 1 H); 4.42–4.40 (*m*, 1 H); 3.76 (*s*, 3 H); 3.37 (*dd*, *J* = 12.1, 4.5, 1 H); 3.07 (*ddd*, *J* = 12.3, 1.6, 1.6, 1 H); 2.20 (*dddd*, *J* = 13.3, 7.5, 1.6, 1.6, 1 H); 2.09 (*ddd*, *J* = 13.3, 10.9, 4.5, 1 H). ^{13}C-NMR (75 MHz, (D_6)DMSO): 168.89 (*s*); 68.29 (*d*); 57.31 (*q*); 52.91 (*t*); 52.87 (*d*); 36.88 (*t*). CI-MS (NH_3): 146.2 (100, $[M + H]^+$).

Methyl (2S,4R)-N-[(tert-Butoxy)carbonyl]-4-hydroxyprolinate (**8**). To the foregoing product (39.0 g, 214.7 mmol) in CH_2Cl_2 (400 ml) was added Et_3N (62.9 g, 621.7 mmol) and a soln. of di(*tert*-butyl) dicarbonate (51.6 g, 236.4 mmol) in CH_2Cl_2 (100 ml). Following the addition of 4-(dimethylamino)pyridine (2.62 g, 21.5 mmol), the mixture was stirred for 3 h at r.t. The clear soln. was washed with 10% citric acid (3 × 300 ml), sat. aq. $NaHCO_3$ soln. (2 × 200 ml), and H_2O (200 ml) and evaporated: **8** (47.0 g, 89%). Yellow oil that was used without further purification. $[\alpha]_D^{25} = -51.0$ ($c = 1.0$, MeOH). IR ($CHCl_3$): 3440*w* (br.), 3010*m*, 2980*m*, 2950*m*, 1745*s*, 1690*s*. ^{1}H-NMR (300 MHz, $CDCl_3$): 4.49–4.37 (*m*, 2 H); 3.73 (*s*, 3 H); 3.67–3.43 (*m*, 2 H); 2.44–2.27 (*m*, 1 H); 2.17–2.02 (*m*, 1 H); 1.87 (br. *s*, 1 H); 1.46, 1.41 (*s*, 9 H). CI-MS: 246.1 (13, $[M + H]^+$), 190.1 (100), 146.1 (12.8).

Methyl (2S,4S)-4-Phthalimidoprolinate–Trifluoroacetic Acid (**9**). To **8** (45.0 g, 183.5 mmol), phthalimide (26.9 g, 182.9 mmol), and PPh_3 (51.6 g, 196.7 mmol) in dry THF (800 ml), diethyl azodicarboxylate (35.1 g, 201.6 mmol) was added dropwise within 20 min. The mixture was stirred for 5.5 h at r.t. After evaporation to *ca.* 100 ml *in vacuo*, the resulting oil was diluted with Et_2O (600 ml) and washed with 5% aq. NaH_2PO_4 (2 × 159 ml) and sat. aq. $NaHCO_3$ soln. (2 × 200 ml). The org. layer was dried (Na_2SO_4) and evaporated to give a product that was used without further purification. After treatment with 10% CF_3COOH/CH_2Cl_2 (500 ml) for 3 h, evaporation gave a yellow viscous oil. Trituration with Et_2O (200 ml) at –20° for 3 d and thorough washing of the precipitate with ice-cold Et_2O afforded colourless crystalline **9** (34.9 g, 49%). M.p. 101–102°. $[\alpha]_D^{25} = +21.1$ ($c = 1.0$, CH_2Cl_2). IR ($CHCl_3$): 3480*w*, 3200*w*, 3030*m*, 3010*m*, 1780*s*, 1750*s*, 1715*s*, 1675*s*. ^{1}H-NMR (300 MHz, $CDCl_3$): 7.88–7.83 (*m*, 2 H); 7.82–7.75 (*m*, 2 H); 5.21 (*dddd*, $J = 9.6, 7.9, 4.8, 4.8$, 1 H); 4.80 (*dd*, $J = 10.3, 7.6$, 1 H); 3.90 (*s*, 3 H); 3.88 (*dd*, $J = 12.6, 7.8$, 1 H); 3.80 (*dd*, $J = 12.6, 4.8$, 1 H); 3.02 (*ddd*, $J = 14.4, 10.2, 9.8$, 1 H); 2.54 (*ddd*, $J = 14.3, 7.6, 5.0$, 1 H). ^{13}C-NMR (75 MHz, $CDCl_3$): 168.93 (*s*); 167.74 (*s*); 134.75 (*d*); 131.36 (*s*); 123.09 (*d*); 58.72 (*d*); 53.72 (*q*); 48.64 (*t*); 47.61 (*d*); 32.69 (*t*). CI-MS (NH_3): 275.1 (100, $[M + H]^+$). Anal. calc. for $C_{16}H_{15}F_3N_2O_6$ (388.30): C 49.49, H 3.89, N 7.21; found: C 49.79, H 4.05, N 7.32.

Methyl (2S,4S,2'S)-1-[N^2-(Benzyloxycarbonyl)-O^1-(tert-butyl)aspart-4-yl]-4-phthalimidoprolinate (**10**). To **9** (12.4 g, 32.0 mmol), Z-Asp(^{t}Bu)-OH (12.0 g, 37.1 mmol), BtOH (4.40 g, 28.7 mmol), and ^{i}Pr$_2$EtN (8.68 g, 67.2 mmol) in DMF (55 ml), HBTU (14.3 g, 37.7 mmol) was added at 0° in three portions. After stirring for 4.5 h at r.t., the mixture was diluted with AcOEt (600 ml) and the soln. washed twice with sat. aq. $NaHCO_3$ (200 ml) and 5% aq. NaH_2PO_4 soln. (200 ml), dried (Na_2SO_4), and evaporated: **10** (16.92 g, 91%) which was used without further purification. Anal. pure **10** was obtained after FC (hexane/AcOEt 5:3, R_f 0.21). M.p. 78°. $[\alpha]_D^{25} = -7.4$ ($c = 1.0$, CH_2Cl_2). IR ($CHCl_3$): 3660*w*, 3420*w*, 3020*m*, 3010*m*, 2980*m*, 2950*m*, 1775*s*, 1720*s*, 1660*m*. ^{1}H-NMR (300 MHz, (D_6)DMSO): 7.90–7.83 (*m*, 4 H); 7.80 (*d*, $J = 8.1$, 1 H); 7.37–7.29 (*m*, 5 H); 5.08–4.99 (*m*, 2 H); 4.89–4.78 (*m*, 1 H); 4.68–4.60 (*m*, 1 H); 4.44 (*dd*, $J = 8.6, 8.6$, 1 H); 4.13 (*dd*, $J = 9.0, 9.0$, 1 H); 3.99 (*dd*, $J = 10.1, 10.1$, 1 H); 3.65 (*s*, 3 H); 2.64–2.44 (*m*, 4 H); 1.39 (*s*, 9 H). ^{13}C-NMR (75 MHz, (D_6)DMSO): 171.26 (*s*); 169.14 (*s*); 168.65 (*s*); 167.55 (*s*); 155.71 (*s*); 136.78 (*s*); 134.43 (*d*); 131.41 (*s*); 128.26 (*d*); 127.75 (*d*); 127.66 (*d*); 122.99 (*d*); 80.36 (*s*); 65.55 (*t*); 57.22 (*d*); 51.81 (*q*); 49.14 (*d*); 47.60 (*d*); 46.42 (*t*); 36.93 (*t*); 29.86 (*t*); 27.54 (*q*). CI-MS (NH_3): 597.4 (7, $[M + NH_4]^+$), 580.4 (100, $[M + H]^+$), 524.3 (27).

tert-*Butyl (3S,7S,8aS)-Perhydro-1,4-dioxo-7-phthalimidopyrrolo[1,2-a]pyrazine-3-acetate*. The foregoing dipeptide (16.8 g, 29.0 mmol) was stirred in DMF (300 ml) with 10% Pd/C (3 g) over 1.5 d under H_2. Additional 10% Pd/C (0.5 g) was then added and stirring was continued for another 2 d. The mixture was filtered through *Celite*, the filtrate evaporated, and the product (9.81 g, 82%) recrystallized from AcOEt. M.p. 196–197°. $[\alpha]_D^{25} = -44.3$ ($c = 1.0$, CH_2Cl_2). IR ($CHCl_3$): 3380*w* (br.), 3020*m*, 3010*m*, 2980*m*, 2930*m*, 1775*m*, 1715*s*, 1680*s*. ^{1}H-NMR (300 MHz, $CDCl_3$): 7.84 (*dd*, $J = 5.5, 3.0$, 2 H); 7.74 (*dd*, $J = 5.5, 3.0$, 2 H); 6.78 (br. *s*, 1 H); 5.01 (*dddd*, $J = 8.7, 8.5, 7.8, 6.2$, 1 H); 4.46 (*dddd*, $J = 10.1, 3.5, 1.6, 0.6$, 1 H); 4.35 (*ddd*, $J = 9.6, 7.8, 1.6$, 1 H); 4.18 (*dd*, $J = 12.3, 6.2$, 1 H); 3.71 (*dd*, $J = 12.3, 8.7$, 1 H); 3.26 (*dd*, $J = 17.4, 3.5$, 1 H); 2.89 (*ddd*, $J = 13.2, 9.6, 8.5$, 1 H); 2.66 (*dd*, $J = 17.4, 10.1$, 1 H); 2.66 (*ddd*, $J = 13.1, 7.8, 7.8$, 1 H); 1.49 (*s*, 9 H). ^{13}C-NMR (75 MHz, $CDCl_3$): 170.64 (*s*); 167.94 (*s*); 167.60 (*s*); 163.95 (*s*); 134.35 (*d*); 131.63 (*s*); 123.57 (*d*); 82.14 (*s*); 58.07 (*d*); 52.28 (*d*); 48.20 (*t*); 46.37 (*d*); 37.06 (*t*); 32.13 (*t*); 28.10 (*q*). CI-MS (NH_3): 414.2 (27, $[M + H]^+$), 375.2 (24), 358.2 (100).

tert-*Butyl (3S,7S,8aS)-7-{[(9H-Fluoren-9-yl)methoxycarbonyl]amino}perhydro-1,4-dioxopyrrolo[1,2-a]-pyrazine-3-acetate*. The foregoing product (7.50 g, 18.1 mmol) and hydrazine hydrate (1.06 g, 21.2 mmol) in EtOH (130 ml) were heated to 70° for 4.5 h. The white suspension was filtered off, the filtrate evaporated, and the residue dried *in vacuo*. The product in dioxan (80 ml) and 1M aq. Na_2CO_3 (62 ml) was treated at 0° with a soln. of Fmoc-Cl (5.80 g, 22.4 mmol) in dioxan (20 ml). The mixture was allowed to warm to r.t. overnight, then diluted with AcOEt (800 ml), and washed with sat. aq. $NaHCO_3$ soln. (2 × 300 ml). After drying (Na_2SO_4) and evaporation *in vacuo*, purification by FC (4% $MeOH/CH_2Cl_2$, R_f 0.28) gave the Fmoc-protected ester (8.62 g, 94%). M.p. 186–187°. $[\alpha]_D^{25} = -45.4$ ($c = 1.1$, DMF). IR (KBr): 3460*w* (br.), 3370*m*, 3330*m*, 3070*w*, 2970*w*, 2930*w*, 2890*w*, 1720*s*, 1695*s*, 1680*s*. ^{1}H-NMR (300 MHz, $CDCl_3$): 7.76 (*d*, $J = 7.4$, 2 H); 7.55 (*d*, $J = 7.3$, 2 H); 7.39 (*t*, $J = 7.4$, 2 H); 7.30 (*t*, $J = 7.4$, 2 H); 6.56 (br. *s*, 1 H); 5.26 (*d*, $J = 5.8$, 1 H); 4.40–4.32 (*m*, 4 H); 4.22–4.17 (*m*, 2 H); 3.72–3.63 (*m*, 2 H);

3.06 (*dd*, J = 17.2, 3.7, 1 H); 2.68–2.61 (*m*, 2 H); 2.26–2.19 (*m*, 1 H); 1.45 (*s*, 9 H). ^{13}C-NMR (75 MHz, $CDCl_3$): 170.21 (*s*); 168.51 (*s*); 164.66 (*s*); 155.85 (*s*); 143.79 (*s*); 141.36 (*s*); 127.78 (*d*); 127.13 (*d*); 125.00 (*d*); 120.03 (*d*); 82.38 (*s*); 67.00 (*t*); 57.61 (*d*); 52.24 (*d*); 51.49 (*t*); 48.72 (*d*); 47.21 (*d*); 36.48 (*t*); 34.42 (*t*); 28.09 (*q*). ES-MS: 528.2 ($[M + Na]^+$).

(3S,7S,8aS)-7-{[(9H-Fluoren-9-yl)methoxycarbonyl]amino}perhydro-1,4-dioxopyrrolo[1,2-a]pyrazine-3-acetic Acid (**4**). The foregoing product (3.0 g, 5.9 mmol) was treated with 5% H_2O in CF_3COOH for 2 h and then evaporated *in vacuo*. The resulting oil was lyophilized from dioxan to give crude **4** that was used for peptide synthesis without further purification. Anal. pure **4** was obtained by HPLC (C_{18} column, 40–80% MeOH/H_2O + 0.1% CF_3COOH over 30 min). M.p. (dec.) > 220°. $[\alpha]_D^{25} = -61.1$ (c = 1.1, DMF). IR (KBr): 3420*m* (br.), 3290*m*, 3060*w*, 3030*w*, 2950*w*, 2880*w*, 1715*s*, 1690v*s*, 1550*s*. ^{1}H-NMR (300 MHz, (D_6)DMSO): 8.21 (br. *s*, 1 H); 7.89 (*d*, J = 7.4, 2 H); 7.68 (*d*, J = 7.3, 2 H); 7.59 (*d*, J = 6.8, 1 H); 7.42 (*t*, J = 7.3, 2 H); 7.34 (*t*, J = 7.3, 2 H); 4.39–4.32 (*m*, 4 H); 4.25–4.11 (*m*, 2 H); 3.59 (*dd*, J = 11.4, 8.1, 1 H); 3.16 (*dd*, J = 11.4, 8.0, 1 H); 2.71 (*dd*, J = 17.2, 6.4, 1 H); 2.57 (*dd*, J = 17.2, 5.3, 1 H); 2.32 (*ddd*, J = 12.7, 6.8, 6.8, 1 H); 1.94–1.83 (*m*, 1 H). ^{13}C-NMR (75 MHz, (D_6)DMSO): 171.79 (*s*); 169.44 (*s*); 165.74 (*s*); 156.17 (*s*); 144.19 (*s*); 141.13 (*s*); 128.00 (*d*); 127.47 (*d*); 125.49 (*d*); 120.48 (*d*); 65.80 (*t*); 57.83 (*d*); 51.59 (*d*); 49.62 (*t*); 48.46 (*d*); 47.08 (*d*); 34.45 (*t*); 33.81 (*t*). ES-MS: 448.4 ($[M - 1]^+$). Anal. calc. for $C_{24}H_{23}N_3O_6$ (449.46): C 64.14, H 5.16, N 9.35; found: C 63.92, H 4.95, N 9.29.

Cyclo(-Ala-Asn-Pro-Asn-Ala-Ala-Temp-) (**5**). Solid-phase peptide synthesis was performed on 0.32 mmol of *Sasrin* resin [18] (*Bachem*; 0.6 mmol/g) pre-loaded with Fmoc-Ala. To this was coupled sequentially Fmoc-Asn(Mtt)-OH, Fmoc-Pro-OH, Fmoc-Asn(Mtt)-OH, Fmoc-Ala-OH, **4**, and Fmoc-Ala-OH (1 mmol each), using BtOH/HBTU for activation. The completion of each coupling cycle was monitored by ninhydrin or isatin tests [46] [47]. Upon assembly of the peptide, the N-terminal Fmoc-protecting group was removed with 20% piperidine/NMP, and the resin was washed with MeOH and CH_2Cl_2. Cleavage of the peptide from the resin (700 mg) was repeated three times each with 1% CF_3COOH/CH_2Cl_2 for 3 min. The combined filtrate was neutralized with sat. aq. $NaHCO_3$ soln., dried (Na_2SO_4), and evaporated to give linear, protected peptide (316 mg, 89%) after purification by HPLC (C_{18} column, 30–100% MeCN/H_2O +0.1% CF_3COOH over 20 min). ES-MS: 1301.3 ($[M + Na]^+$), 1279.3 ($[M + H]^+$), 662.1 ($[M + 2\,Na]^{2+}$).

For cyclization, the linear peptide (200 mg, 0.16 mmol) in 1% ^{i}Pr$_2$EtN/DMF was stirred with a three-fold excess of BtOH and TPTU for 2 h at 0° and then overnight at r.t. Evaporation and purification by HPLC (C_{18} column, 35–95% MeCN/H_2O +0.1% CF_3COOH over 20 min) afforded side-chain-protected cyclopeptide (58 mg, 29%). ES-MS: 1299.5 ($[M + K]^+$), 1283.3 ($[M + Na]^+$), 1261 ($[M + H]^+$), 661.3 ($[M + Na + K]^{2+}$), 653.2 ($[M + 2\,Na]^{2+}$).

The protected cyclopeptide was treated with 5% triisopropylsilane in CF_3COOH for 1 h at r.t. Evaporation, titration with ^{i}Pr$_2$O, and purification by HPLC (C_{18} column 0–30% MeCN/H_2O +0.1% CF_3COOH over 20 min) gave **5** (55%). ^{1}H-NMR (600 MHz, $^2H_2O/H_2O$ 1:9, pH 5.0, 300 K): *Table 1*. ES-MS: 786.5 ($[M + K]^+$), 770.7 ($[M + Na]^+$), 394.0 ($[M + H + K]^{2+}$). Amino-acid analysis (molar ratio): Ala 3.00, Asp 2.74, Pro 1.00, ((2*S*, 4*S*)-4-aminoproline not determined).

Cyclo(-Ala-Arg-Gly-Asp-Temp-) (**6**). Fmoc-Ala-OH (4 × excess) was coupled to *Sasrin* resin (*Bachem*) using dicyclohexylcarbodiimide (DCC)/4-(dimethylamino)pyridine for activation in NMP. The synthesis was performed on 0.20 mmol by chain elongation with **4**, Fmoc-Asp(^{t}Bu)-OH, Fmoc-Gly-OH and Fmoc-Arg(Pmc)-OH (1 mmol each) and HBTU/BtOH for activation. After completion of the synthesis, the peptide was cleaved from the resin as described above. Purification by HPLC (C_{18} column, 30–80% MeCN/H_2O +0.1% CF_3COOH over 20 min) afforded side-chain protected linear peptide (171 mg, 90%): ES-MS: 972.1 ($[M + Na]^+$), 950.3 $[M + H]^+$).

After cyclization, as above, purification by HPLC (C_{18} column, 55–100% MeCN/H_2O +0.1% CF_3COOH over 20 min) gave protected cyclopeptide (102 mg, 69%). ES-MS: 954.4 ($[M + Na]^+$), 488.8 ($[M + 2\,Na]^{2+}$).

The protected cyclopeptide (85 mg, 0.09 mmol), was treated with CF_3COOH/thioanisole/EDT/anisole 90:5:3:2 (30 ml) for 2 h. Evaporation, trituration with ^{i}Pr$_2$O, and purification by HPLC (C_{18} column, 0–30% MeCN/H_2O +0.1% CF_3COOH over 20 min) gave **6** (45 mg, 81%). ^{1}H-NMR (600 MHz, $^2H_2O/H_2O$ 1:9, pH 5.0, 300 K): *Table 2*. ES-MS: 609.9 ($[M + H]^+$). Amino-acid analysis (molar ratio): Ala 1.00, Arg 0.99, Asp 2.00, Gly 1.03 ((2*S*,4*S*)-4-aminoproline not determined).

Structure Calculations. The ROE connectivities were used to derive distance restraints as input for structure calculations using the simulated annealing (SA) protocol [37] with the DISCOVER program (*Biosym*, San Diego) and the CVFF force field. Cross-peak volumes were quantitated in ROESY spectra with 75, 150, 225, 300 and 375 ms mixing times (spin lock) using the FELIX software (*Biosym*, San Diego) and were corrected for resonance offset effects, as described by *Griesinger* and *Ernst* [48] for medium-size molecules. Distances were calibrated using $d(\alpha^1,NH^2)$ (Ala^1-Asn^2) and $d(\beta^2,\beta'^2)$ (Asn^2) distances of 2.3 and 1.75 Å, respectively, and calculating other distances according to the r^{-6} relationship, using three models; 1) assuming a linear NOE build-up to 225 ms

mixing time and using the cross-peak volumes at 225 ms to determine distances; 2) fitting a straight line to the build-up curve, from which distances were then extracted; 3) fitting the build-up curve to a second-order polynomial function. The agreement between the distances calculated in these ways was excellent, indicating the absence of spin diffusion effects in the ROE's used. Distances determined in this way to be $\leqslant 2.5$ Å were set to 2.7, those > 2.5 Å but $\leqslant 3.0$ Å were set at 3.2 Å, and those > 3.0 Å were set as 5.0 Å. The necessary pseudoatom corrections [28] were applied for non-stereospecifically assigned protons at prochiral centres and for Me groups, and the resulting values were used as input upper distance restraints. NOE Restraint violations were penalized with a weighting factor of 15 kcal/mol/Å with an upper limit of 250 kcal/mol/Å.

The calculations were initiated with an arbitrary starting conformation. Typically, 30–50 calculations were performed differing in the values of the random number seed, to generate different initial velocities for all atoms. Each calculation then consisted of initial energy minimization (100 steps steepest descent), 45 ps of molecular dynamics at 1000 K, during which first the NOE force constants, and then the internal force constants were scaled-up, 15 ps of molecular dynamics during cooling to 300 K, energy minimization (100 steps steepest descent, 100 steps conjugate gradient, 100 steps quasi-*Newton-Raphson*), 5 ps molecular dynamics at 300 K, and a final energy minimization (100 steps steepest descent, 100 steps conjugate gradient, 1000 steps quasi-*Newton-Raphson*). The *van der Waals* potential was set to a quartic form during the SA procedure and changed to the normal *Lennard-Jones* potential for final energy minimization. A cutoff distance of 10 Å for nonbonded interactions was used. Charges and cross terms were not included during dynamics, but in the final stages of minimization both were included, using a distance-dependent dielectric scaled by a factor of $4 \cdot r$. Constraints were applied to avoid inversions at chiral centres and the conversion of *trans* to *cis* peptide bonds or *vice versa*.

REFERENCES

[1] K.D. Kopple, P.W. Baures, J.W. Bean, C.A. D'Ambrosio, J.L. Hughes, C.E. Peishoff, D.S. Eggleston, *J. Am. Chem. Soc.* **1992,** *114,* 9615.

[2] C.D Eldred, B. Evans, S. Hindley, B.D. Judkins, H.A. Kelly, J. Kitchin, P. Lumley, B. Porter, B.C. Ross, K.J. Smith, N.R. Taylor, J.R. Wheatcroft, *J. Med. Chem.* **1994,** *37,* 3882.

[3] A.C. Bach, C.J. Eyermann, J.D. Gross, M.J. Bower, R.L. Harlow, P.C. Weber, W.F. DeGrado, *J. Am. Chem. Soc.* **1994,** *116,* 3207.

[4] R.S. McDowell, T.R. Gadek, P.L. Barker, D.J. Burdick, K.S. Chan, C.L. Quan, N. Skelton, M. Struble, E.D. Thorsett, M. Tischler, J.Y.K. Tom, T.R. Webb, J.P. Burnier, *J. Am. Chem. Soc.* **1994,** *116,* 5069.

[5] S. Jackson, W.F. DeGrado, A. Dwivedi, A. Parthasarathy, A. Higley, J. Krywko, A. Rockwell, J. Markwalder, G. Wells, R. Wexler, S. Mousa, R. Harlow, *J. Am. Chem. Soc.* **1994,** *116,* 3220.

[6] A.C. Bach, J.R. Espina, S.A. Jackson, P.F.W. Stouten, J.L. Duke, S.A. Mousa, W.F. DeGrado, *J. Am. Chem. Soc.* **1996,** *118,* 293.

[7] F. Brown, *Philos. Trans. R. Soc. Lond.* **1994,** *344,* 213.

[8] E. Riley, *Curr. Opin. Immunol.* **1995,** *7,* 612.

[9] A. Moreno, M.E. Patarroyo, *Curr. Opin. Immunol.* **1995,** *7,* 607.

[10] M.K. Hart, T.J. Palker, B.F. Haynes, in 'Vaccine Design', 'Pharmaceutical Biotechnology, Vol.6', Eds. M.F. Powell and M.J. Newman, Plenum Press, New York, 1995, p.821.

[11] D.A. Harn, S.R. Reynolds, S. Chikunguwo, S. Furlong, C. Dahl, in 'Vaccine Design', 'Pharmaceutical Biotechnology, Vol. 6', Eds. M.F. Powell and M.J. Newman, Plenum Press, New York, 1995, p.891.

[12] F. Brown, *Vaccine* **1992,** *10,* 1022.

[13] J.C. Herr, *Am. J. Reprod. Immunol.* **1996,** *35,* 184.

[14] H.J. Dyson, A.C. Satterthwait, R.A. Lerner, P.E. Wright, *Biochemistry* **1990,** *29,* 7828.

[15] C. Bisang, C. Weber, J. Inglis, C.A. Schiffer, W.F. van Gunsteren, I. Jelesarov, H.R. Bosshard, J.A. Robinson, *J. Am. Chem. Soc.* **1995,** *117,* 7904.

[16] S. Zinn-Justin, C. Roumestand, B. Gilquin, F. Bontems, A. Ménez, F. Toma, *Biochemistry* **1992,** *31,* 11335.

[17] O. Mitsunobu, M. Wada, T. Sano, *J. Am. Chem. Soc.* **1972,** *94,* 679.

[18] M. Megler, R. Tanner, J. Gosteli, P. Grogg, *Tetrahedron Lett.* **1988,** *29.* 4005.

[19] R. Knorr, A. Trzeciak, W. Bannwarth, D. Gillessen, *Tetrahedron Lett.* **1989,** *30,* 1927.

[20] P. Güntert, W. Braun, M. Billeter, K. Wüthrich, *J. Am. Chem. Soc.* **1989,** *111,* 3997.

[21] M.P. Williamson, *Biopolymers* **1990,** *29,* 1423.

[22] D.S. Wishart, B.D. Sykes, F.M. Richards, *J. Mol. Biol.* **1991,** *222,* 311.

[23] T. Asakura, K. Taoka, M. Demura, M.P. Williamson, *J. Biomol. NMR* **1995,** *6,* 227.

[24] G. Merutka, H.J. Dyson, P.E. Wright, *J. Biomol. NMR* **1995,** *5,* 14.
[25] S.W. Englander, L. Mayne, *Annu. Rev. Biophys. Biomol. Struct.* **1992,** *21,* 243.
[26] S.W. Englander, N.R. Kallenbach, *Quart. Revs. Biophys.* **1984,** *16,* 521.
[27] M. Eberstadt, G. Gemmecker, D.F. Mierke, H. Kessler, *Angew. Chem. Int. Ed.* **1995,** *35,* 167.
[28] K. Wüthrich, 'NMR of Proteins and Nucleic Acids', Wiley-Interscience, New York, 1986.
[29] I. Karle, *J. Am. Chem. Soc.* **1972,** *94,* 81.
[30] F.A.A.M. de Leeuw, C. Altona, H. Kessler, W. Bermel, A. Friedrich, G. Krack, W.E. Hull, *J. Am. Chem. Soc.* **1983,** *105,* 2237.
[31] J.J.M. Sleeckx, M.J.O. Anteunis, *Bull. Soc. Chim. Belg.* **1985,** *94,* 187.
[32] A. Demarco, M. Llinas, K. Wüthrich, *Biopolymers* **1978,** *17,* 617.
[33] Z.L. Mádi, C. Griesinger, R.R. Ernst, *J. Am. Chem. Soc.* **1990,** *112,* 2908.
[34] M. Cai, Y. Huang, J. Liu, R. Krishnamoorthi, *J. Biomol. NMR* **1995,** *6,* 123.
[35] D.B. Davies, M.A. Khaled, *J. Chem. Soc., Perkin Trans. 1* **1976,** 1238.
[36] F.S. Reyniers, F.A.M. Borremans, M.J.O. Anteunis, *Bull. Soc. Chim. Belg.* **1985,** *94,* 413.
[37] M. Nilges, A.M. Gronenborn, A.T. Brünger, G.M. Clore, *Protein Eng.* **1988,** *2,* 27.
[38] E.G. Hutchinson, J.M. Thornton, *Protein Sci.* **1994,** *3,* 2207.
[39] J. Reed, W.E. Hull, C.-W. Lieth, D. Kübler, S. Suhai, V. Kinzel, *Eur. J. Biochem.* **1988,** *178,* 141.
[40] N.H. Andersen, C. Chen, T.M. Marschner, S.R. Krystek, D.A. Bassolino, *Biochemistry* **1992,** *31,* 1280.
[41] K.J. Nielsen, D. Alewood, J. Andrews, S.B.H. Kent, D.J. Craik, *Protein Sci.* **1994,** *3,* 291.
[42] K.J. Nielsen, R.L. Heath, M.A. Anderson, D.J. Craik, *Biochemistry* **1995,** *34,* 14304.
[43] L. Alig, A. Edenhofer, P. Hadváry, M. Hürzeler, D. Knopp, M. Müller, B. Steiner, A. Trzeciak, T. Weller, *J. Med. Chem.* **1992,** *35,* 4393.
[44] F. Emery, C. Bisang, M. Favre, L. Jiang, *J. Chem. Soc., Chem. Comm.* **1996,** in press.
[45] D. Gramberg, C. Weber, R. Beeli, J. Inglis, C. Bruns, J.A. Robinson, *Helv. Chim. Acta* **1995,** *78,* 1588.
[46] V.K. Sarin, S.B.H. Kent, J.P. Tam, R.B. Merrifield, *Anal. Biochem.* **1981,** *117,* 147.
[47] E. Kaiser, C.D. Bossinger, R.L. Colescott, D.B. Olsen, *Anal. Chim. Acta* **1980,** *118,* 149.
[48] C. Griesinger, R.R. Ernst, *J. Magn. Reson.* **1987,** *75,* 261.